The Energy Cost of Artificial Intelligence of Things Lifecycle

Shih-Kai Chou, Jernej Hribar, Mihael Mohorčič and Carolina Fortuna

Department of Communication Systems, Jožef Stefan Institute, Slovenia

Email:{shih-kai.chou, jernej.hribar, miha.mohorcic, carolina.fortuna}@ijs.si

Abstract—**Artificial Intelligence (AI) coupled with existing Internet of Things (IoT) enables more streamlined and autonomous operations across various economic sectors. Consequently, the paradigm of Artificial Intelligence of Things (AIoT) having AI techniques at its core implies additional energy and carbon costs that may become significant with more complex neural architectures. To better understand the energy and Carbon Footprint (CF) of some AIoT components, very recent studies employ conventional metrics. However, these metrics are not designed to capture energy efficiency aspects of inference. In this paper, we propose a new metric, the Energy Cost of AIoT Lifecycle (eCAL) to capture the overall energy cost of inference over the lifecycle of an AIoT system. We devise a new methodology for determining eCAL of an AIoT system by analyzing the complexity of data manipulation in individual components involved in the AIoT lifecycle and derive the overall and per bit energy consumption. With eCAL we show that the better a model is and the more it is used, the more energy efficient an inference is. For an example AIoT configuration, eCAL for making 100 inferences is 1.43 times higher than for 1000 inferences. We also evaluate the CF of the AIoT system by calculating the equivalent CO_2 emissions based on the energy consumption and the Carbon Intensity (CI) across different countries. Using 2023 renewable data, our analysis reveals that deploying an AIoT system in Germany results in emitting 4.62 times higher CO_2 than in Finland, due to latter using more low-CI energy sources.**

Index Terms—**AIoT lifecycle, Energy Consumption, Carbon Footprint, Metric, Methodology**

I. INTRODUCTION

Next-generation networks aim to deliver unprecedented levels of connectivity and intelligence, facilitating seamless interactions between a massive number of devices, services, and applications. The trend is especially noticeable in Internet of Things (IoT) where devices are becoming increasingly more intelligent [1], from smart home appliances [2] to industrial machinery [3], Smart City [4], vehicle-to-everything (V2X) [5], and beyond [6], [7]. With the help of Artificial Intelligence (AI), we are moving away from conventional IoT applications towards Artificial Intelligence of Things (AIoT) systems [8] designed to achieve more streamlined and autonomous operations. For example, in future smart factories, the integration of AI and IoT will enable real-time monitoring and optimization of production processes, predictive maintenance, and enhanced decision-making capabilities.

While AIoT systems enable unprecedented automation and agility, their reliance on AI implies additional energy and carbon costs [9]. Especially in the cases when models with many parameters are employed, such as Large language model (LLM)s, such costs may be significant [10]. In light of climate challenges, the general AI research community's effort to better estimate the costs of training [11], estimate the cost of AI [12], the Carbon Footprint (CF)s of LLMs [13] and find ways to scale models efficiently [14] are intensifying. Furthermore, the networking and IoT communities increasingly relying on AI techniques are also investigating pathways towards [15] net-zero carbon emissions, analyzing the CF of various learning techniques [16] and data modalities while also developing various approaches to optimizing energy efficiency through hardware-software optimization [17], scheduling [18], more efficient model design [19] and energy and carbon consumption testing [20].

Depending on the scope of the study, various metrics are employed to understand energy and CF. For instance, [17] considers normalized energy as well as energy for buffering in $[J]$, energy $[Wh]$ and $[CO_2eq]$ for the various phases involved in federated learning (FL) edge systems [15], [16], $[J]$ and GFLOPS of the neural architectures [19] and energy $[Wh]$ for the scheduled loads in [18]. However, these metrics are not specifically designed to capture the energy efficiency of a system or part of. As well noted in [15], the traditional ITU standardized Energy-per-Bit $[J/b]$ metric *'will no longer be able to reflect the environmental impact of the modern mobile services, especially network AI-enabled smart services'*.

Recently, a number of environmentally friendly metrics, such as accuracy per consumption (APC), that capture the performance of a AI model together with its environmental impact [21]. Nevertheless we observe the following. First, while the metrics proposed in [21] are powerful in terms of assessing the energy/performance tradeoffs of models, these metrics are less suitable in assessing the energy efficiency of a system such as AIoT. Second, that a metric somewhat similar to the Energy-per-Bit $[J/b]$ would be more suitable for measuring energy efficiency. Third, other efficiency metrics have been proposed in wireless in particular and engineering and economy in general [22]. For instance, spectral efficiency, measured in $[b/s/Hz]$ [23] provides a means of calculating the amount of data bandwidth available in a given amount of spectrum, while lifecycle emissions for vehicles, measured in $[g/km]$ [24], enables computing the CF in grams per kilometer.

Following these observations, in this paper, we aim to find a suitable energy efficiency metric that would be simple, general and holistically quantify the environmental cost of inference

carried out in AIoT systems. The contributions of this paper are as follows:

- We propose a new metric, the Energy Cost of AIoT Lifecycle (eCAL), also measured in $[J/b]$, that captures the overall energy cost of generating an inference in an AIoT system. Unlike capturing the energy required for transmitting bits that is done by the Energy-per-Bit $[J/b]$ metric, or $[J]$ for AI model complexity, the proposed eCAL captures the energy consumed by all the data manipulation components in an AIoT system during the lifecycle of a trained model enabling inference.
- We devise a methodology for determining the eCAL of an AIoT system. The methodology breaks down the AIoT system into different data manipulation components, i.e. data collection, storage, and data preprocessing, training along with evaluation, and inference, and, for each component, it analyzes the complexity of data manipulation and derives the overall and per bit energy consumption.
- Using the proposed metric, we show that the better a model is and the more it is used, the more energy efficient an inference is. For an example AIoT configuration, the energy consumption per bit for making 100 inferences is 1.33 times higher than for 1000 inferences. This can be explained by the fact that the energy cost of data collection, storage, training and evaluation, all necessary to develop an AI model are spread across more inferences.
- We evaluate the CF of the AIoT system by calculating the equivalent CO_2 emissions based on the energy consumption and the Carbon Intensity (CI) across different countries. Using 2023 renewable data, our analysis reveals that deploying an AIoT system in Germany results in emitting 4.62 times higher CO_2 than in Finland, due to the latter using more low-CI energy sources.

The paper is structured as follows. We first review the relevant literature in Section II, we then describe the lifecycle of an AIoT system, define eCAL and the methodology for deriving it in Section III. Subsequently, the derivation of the energy consumption formulas for different data manipulation components involved in the AIoT lifecycle are provided in Sections IV to VII. In Section VIII, the proposed metric, eCAL, is derived and analyzed, demonstrating its utility in capturing the overall energy cost of AIoT systems over its lifecycle. whereas in Section IX we discuss the CF aspect of such a system, comparing emissions across different European countries. Finally, Section X concludes the paper and outlines future research directions.

II. RELATED WORKS

While AIoT systems enable unprecedented automation and agility, their reliance on AI implies additional energy and carbon costs [9] that in some cases that employ models with many parameters, such as LLMs, may be significant [10]. In light of climate challenges and the dazzling footprints of the latest generation of LLMs [13], the general AI research community's effort to better understand and then formalize methods to asses the environmental impact of the AI revolution is rising. Due to the complexity of state of the art neural architectures, in many cases the energy cost of training is computed after the training by measuring the performed computation through interfaces such as the performance application programming interface [25]. Furthermore, [11] shows that the energy footprint of inference is more studied than the one for training and highlights below 70% accuracy between predicted and measured energy consumption.

However, a number of approaches and tools capable of proactively estimating the energy and environmental cost of training have also emerged. LLMCarbon [13] is a very recent end-to-end CF projection model designed for both dense and mixture of experts LLMs. It incorporates critical LLM, hardware, and data center parameters, such as LLM parameter count, hardware type, system power, chip area, and data center efficiency, to model both operational and embodied CFs of a LLM. Furthermore, [14] aims at providing guidelines for scaling AI in a sustainable way. They analyze the energy efficiency of new processing units, the CF of the most prominent LLM models since GPT-3 and analyze their lifecycle carbon impact showing that inference and training are comparable. They conclude that, to enable sustainability as a computer system design principle, better tools for carbon telemetry are required, large scale carbon datasets, carbon impact disclosure and more suitable carbon metrics.

The networking and IoT communities, increasingly relying on AI techniques, are also investigating pathways towards [15] net-zero carbon emissions. The authors of [15] notice that in spite of improvements in hardware and software energy efficiency, the overall energy consumption of mobile networks continues to rise, exacerbated by the growing use of resource-intensive AI algorithms. They introduce a novel evaluation framework to analyze the lifecycle of network AI implementations, identifying major emission sources. They propose the Dynamic Energy Trading and Task Allocation framework, designed to optimize carbon emissions by reallocating renewable energy sources and distributing tasks more efficiently across the network. Similar as in [14], they highlight the development of new metrics to quantify the environmental impact of new network services enabled by AI.

The authors of [16] introduce a novel framework to quantify energy consumption and carbon emissions for vanilla FL methods and consensus-based decentralized approaches, identifying optimal operational points for sustainable FL designs. Two case studies are analyzed within 5G industry verticals: continual learning and reinforcement learning scenarios. Together with the authors of [15], they consider energy $[Wh]$ and $[CO_2eq]$ in their evaluations. The solution proposed in [17] is a hardware/software co-design that introduces modality gating (throttling) to adaptively manage sensing and computing tasks. AMG features a novel decoupled modality sensor architecture that supports partial throttling of sensors, significantly reducing energy consumption while maintaining data flow across multimodal data: text, speech, images and video. More energy efficient task scheduling has been considered in [18], while more efficient neural architecture design and subsequent

model development in [19]. The energy efficiency of various programming languages is studied in [26] while energy and carbon consumption testing for AI-driven IoT services is developed in [20].

Novel metrics to evaluate Deep Learning (DL) models, considering not only their accuracy and speed but also their energy consumption and cost have been proposed in [21]. The four metrics are: Accuracy Per Consumption (APC) and Accuracy Per Energy Cost (APEC) for inference, and Time To Closest APC (TTCAPC) and Time To Closest APEC (TTCAPEC) for training. These metrics aim to promote the use of energy-efficient and green energy-powered DL systems by integrating energy considerations into the performance evaluation. Nevertheless, while powerful in terms of assessing the energy/performance tradeoffs of models, these metrics are less suitable in assessing the energy efficiency of a system such as AIoT. The Energy-per-Bit $[J/b]$ has been defined for assessing the efficiency of transmissions and therefore does not capture the AI aspects as also noted in [15]. Looking at the electric vehicle literature, we notice that, when comparing to traditional gas vehicles they employ lifecycle emissions as a metric, measured in $[g/km]$ [24].

Inspired by the simplicity and effectiveness of metrics such as transmission efficiency through energy-per-bit and the lifecycle emissions, and responding to calls for new metrics [14], [15] that capture the energy cost in the era of AI enabled systems, this work proposes the novel Energy Cost of AIoT Lifecycle (eCAL) metric and methodology to derive it.

III. eCAL Definition and Methodology

In our work, we consider an AIoT communication and computing system whose *lifecycle* is depicted in Fig. 1, consisting of the following data manipulating components:

a) Data Collection: This data-manipulating component, depicted in the lower part of Fig. 1, the collected data N_{S}, includes receiving telemetry data from sensors to the terminal computing infrastructure via wired or wireless technologies. The collected information can be turned into indicators such as signal strength, and for example, be interpreted by the AI models to predict the location of a user. To move this data from the sensor to the access point (AP), E_{T} $[J]$ is needed.

b) Storage and Data Preprocessing: Once the data from IoT devices arrives at the computing infrastructure, it is first stored on the hard drive, and then fetched for preprocessing. Therefore, the energy consumption, E_{storage}, of this component arises from reading and writing data N_{S} into the storage units, which can vary depending on data volume and modality. To ensure accuracy and reliability during the training process, the data, N_{S}, must go through several preprocessing steps such as cleaning, feature engineering and transformation. The energy consumption for preprocessing E_{pre}, depends on the integrity of the ingested dataset. For example, datasets with a lot of invalid or missing data, require more extensive cleaning and error correction.
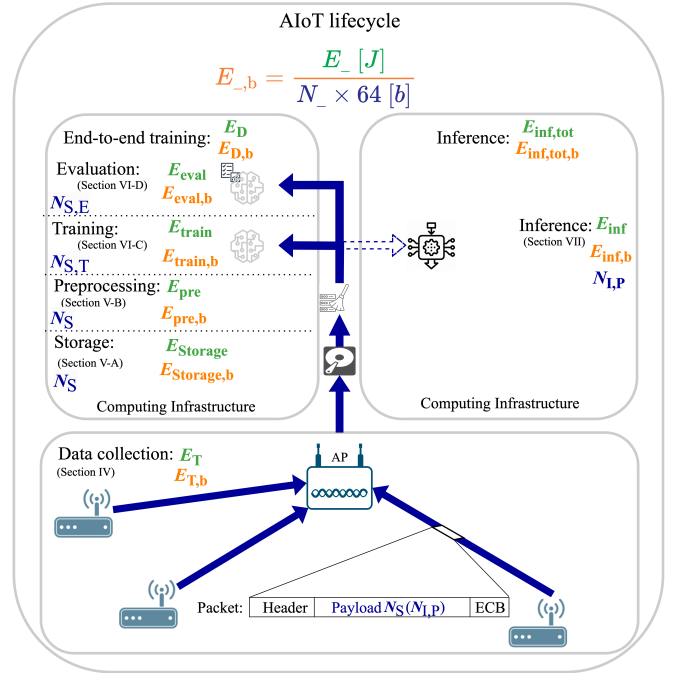

Fig. 1: Data manipulation components involved in the lifecycle of an AIoT system.

c) Training and Evaluation: The training component comprises the model development of the AI/Machine Learning (ML) using selected AI/ML techniques, such as neural architectures, and data. In this step of the model development process, the processed data, $N_{\text{S,T}}$ is fetched and utilized to learn weights and biases in order to approximate the underlying distribution. For most neural architectures, the learning processes rely on Graphics Processing Unit (GPU) and Tensor Processing Unit (TPU) performing complex tensor processing operations and consuming E_{train}. Once the neural architecture weights are learned using the data in view of minimizing a loss function, the model is considered ready for evaluation and deployment. Subsequently, the quality of the learned model is evaluated on the evaluation datasets, $N_{\text{S,E}}$, a process that consumes E_{eval} energy. The data storage, preprocessing, training, and evaluation form the end-to-end training of the AI/ML model and cumulatively require E_{D} energy to complete.

d) Inference: Once the model is trained, it can be used by applications in inference mode. Various applications can send samples of data $N_{\text{I,P}}$ and receive model outputs in the form of forecasts for regression problems or discrete (categorical) for classification problems. The energy consumption E_{inf} of a single inference is relatively small, however for high volumes of requests it can become significant.

Based on this lifecycle, we proposed eCAL as the ratio between all the energy consumed by all data manipulation components and all the manipulated application-level bits:

$$eCAL =$$

$$\frac{\text{Total energy of data manipulation components } [J]}{\text{Total manipulated application level data } [b]}.$$

(1)

In the upcoming sections, we employ the following methodology in order to finally derive the proposed metric. We follow the telemetry data flow, highlighted with blue in Figure 1, across the above-mentioned components and derive the computational complexity and subsequently the absolute and per bit energy consumption, highlighted with green and orange respectively, in each component. For instance, in Section IV, we derive E_T and $E_{T,b}$ for the data collection component while in Section V, we do the same for preprocessing and storage E_{pre} and $E_{pre,b}$ respectively. With this formalism in place, Section VIII is concerned with deriving eCAL.

In addition to providing the first theoretical framework for assessing and quantifying the energy consumption of each component of an AIoT system in the data manipulation workflow, we also discuss and show differences across countries in view of AIoT inference CF.

IV. ENERGY COST OF DATA COLLECTION

In this section, we derive the energy cost of *data collection* in an AIoT system. To calculate the cost, we first determine the number of bits that need to be transmitted from IoT devices to the server via wireless technology. Then we calculate the energy consumption based on the given transmitting power and corresponding transmission rate. In the last step, we derive the total energy consumption for collecting data from IoT devices. The energy consumption of wired communication compared to the wireless part is negligible [29]. Therefore, in this work, we only consider the communication from the IoT device to the AP via wireless technologies.

Each wireless technology relies on different multi-layer protocol stack adding overhead bits, e.g., header, error correction, etc., to ensure collected data integrity and efficient transmission thus increasing energy consumption. Therefore, each packet is composed of payload, e.g., measurements collected by an IoT device, and overhead, with overhead size depending on the selected technology. The size of the transmitted data in bits (B_T) can be expressed as defined in [30]:

$$B_T \ [b] = \underbrace{\alpha N_S}_{\text{payload}} + \underbrace{\lceil \frac{\alpha N_S}{F_U} \rceil \cdot \Omega_U}_{\text{Overhead}},$$

(2)

where α represents bit precision, i.e., the number of bits required to store value of a sample in floating number. Typically α equals 32 bits for single precision (float) or 64 bits for double precision. Moreover, we denote *samples* as N_S which represents the telemetry data that the application requests from the device in floating-point form, i.e., when an application requests 256 *samples*, the payload size can be calculated as 8192 and 16384 bits for single precision and double precision, respectively. The second part of the equation represents the
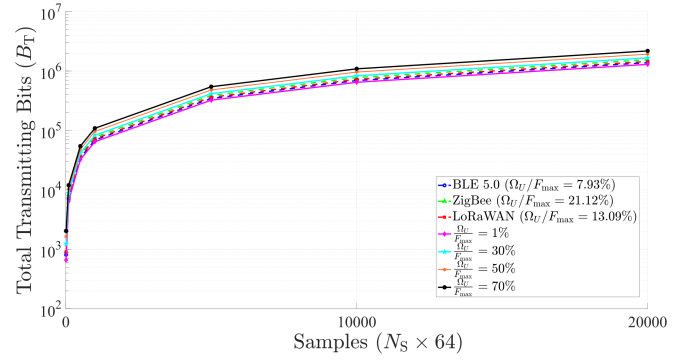

Fig. 2: Number of transmitting data (B_T) versus payload (αN_S).

overhead. First, the number of packets is determined, by rounding up the payload divided with the maximal number of bits in one packet (F_U) for the selected access technology. To obtain the total overhead the number of packets is then multiplied with the number of overhead bits per packet, that also depends on the selected access technology.

To illustrate the behavior of Eq. 2, we consider a scenario of a single device transmitting $N_S = 256$ of double-precision samples to the application and alter the overhead percentages in one packet. More specifically, we consider a fixed packet size of 2000 bits. We consider overhead of 1%, 30%, 50%, and 70%. Additionally, we consider overhead percentages of three mainstream wireless technologies [31] for IoT systems, namely Bluetooth Low Energy (BLE) 5.0 [32], ZigBee [33], and Long Range Wide Area Network (LoRaWAN) [34]. In Table I, we summarize the parameters of these three technologies based on IoT protocol stack, in which the uplink data goes through the physical layer to the application layer. Fig. 2 illustrates the relationship between the number of samples and the size of the transmitted data for different percentages of overhead. As seen in the figure, higher overhead percentages result in significantly more data being sent than when overhead is low. For example, when transferring 256 samples, the data transfer requirements for the scenarios $\Omega_U = 1\% F_U$ and $\Omega_U = 70\% F_U$ are 16564 and 28984 bits, respectively, which means the latter has 1.7 times higher data transfer requirements than the former.

Thus, we can conclude that *when the size of samples (N_S) is small, leveraging wireless technologies with lower overhead, such as BLE, is advantageous. These technologies efficiently transmit fewer total bits. However, as the size of samples increases, the impact of overhead becomes less significant. In these scenarios, technologies with higher overhead but larger maximum packet sizes can become more beneficial. This shift emphasizes the importance of the trade-off between overhead, sample size, and maximum packet size, and highlights the importance of selecting the appropriate technology to achieve adequate energy efficiency in AIoT deployments.*

Next, we determine the energy consumption for a given

4

TABLE I: Different technologies for transmitting 256 double precision samples ($\alpha = 64$ and $N_S = 256$).

Technology	F_U	Number of packets	Ω_U	B_T	$\frac{\Omega_U}{F_U}(\%)$	Included protocol overhead
BLE 5.0 (1 Mbps)	2120	8	168	17728	7.93%	PHY+MAC+Link Layer+ L2CAP+ATT header
ZigBee [27]	1288	13	272	19920	21.12%	IEEE802.15.4 PHY and MAC+Link Layer+APS header
LoRaWAN [28]	2048	9	268	18796	13.09%	PHY+MAC+Link Layer

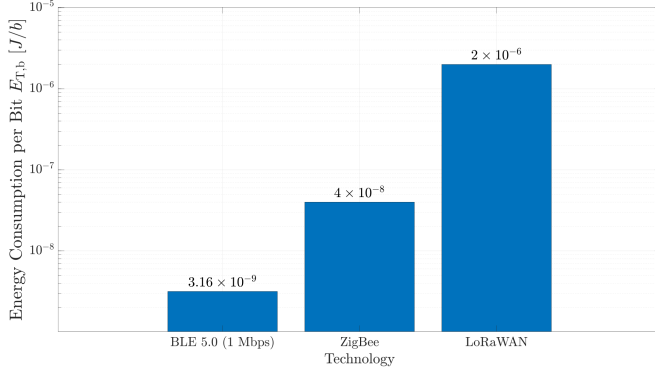
Fig. 3: Energy consumption per bit ($E_{T,b}$) across different technologies.

technology, which we define as follows:

$$E_T[J] = \frac{P_T[W]}{R_T[b/s]} \cdot B_T[b]. \qquad (3)$$

where P_T represents the transmitting power. As a result, we can obtain energy consumption per bit for transmitting part of AIoT system as follows:

$$E_{T,b}[J/b] = \frac{P_T[W] \cdot T_T[s]}{B_T[b]} = \frac{P_T[W]}{R_T[b/s]}, \qquad (4)$$

where T_T is the corresponding transmitting time. T_T can be derived from the corresponding transmitting rate (R_T) and B_T, and is expressed as $T_T = \frac{B_T}{R_T}$.

Considering the previous example, if we transmitted the 256 samples with 1% overhead with $P_T = 10$ [mW] and $R_T = 10^3$ [b/s], the energy consumption [J] of 1% overhead would be 0.165, and 70% is 0.29. Moreover, the energy consumption per bit [J/b] for both 1% overhead and 70% overhead would be 10^{-5}.

We can observe from the above equations that *we are able to determine that when considering energy consumption per bit ($E_{T,b}$), this metric is exclusively related to P_T and R_T, which indicates that the energy required to transmit one bit of data depends on the power used for transmission and the speed of the transmission. Meaning, that energy consumption per bit is the inverse of energy efficiency* [35].

We consider the wireless technologies listed in Table I to illustrate per-bit energy consumption with the corresponding P_T and R_T and calculated $E_{T,b}$ in Table II. The comparison between $E_{T,b}$ of different technologies is shown in Fig. 3. It can be seen that BLE exhibits the best performance due to its low power consumption and high transmission rate, while

TABLE II: Transmitting power (P_T), transmitting rate (R_T), and energy consumption per bit ($E_{T,b}$) for different technologies.

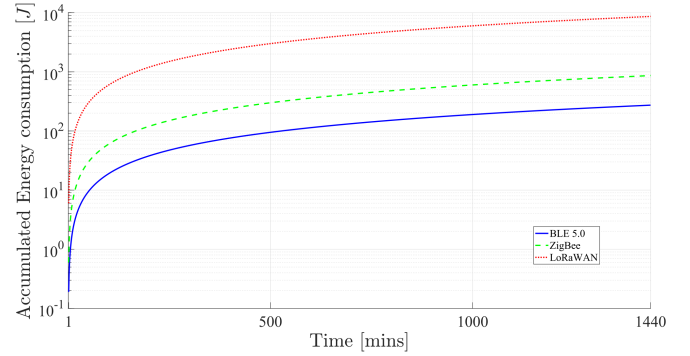|	P_T (mW)	R_T (bit/s)	$E_{T,b}$ (J/b)
BLE 5.0 (1 Mbps)	3.1628	1×10^6	3.1628 nJ/bit
ZigBee [27]	10	250×10^3	40 nJ/bit
LoRaWAN [28]	100	50×10^3	2 μ J/b

Fig. 4: Energy consumption (E_T) over a 24 hours Interval.

LoRaWAN exhibits the highest energy consumption per bit despite its low overhead. This emphasizes the crucial role of transmission power and rate in determining the overall energy efficiency in AIoT systems. Our results underscore the need to evaluate both power consumption and transmission rate, not just overhead, when selecting the communication technology for AIoT deployments. Prioritizing lower power consumption and higher transmission rates can significantly improve energy consumption per bit.

Finally, the total energy consumption of the data transmission in an AIoT system is illustrated in Fig. 4. We assume that the signals are transmitted at one-minute intervals and uniformly. These results showcase the total energy consumption over a period of 24 hours of continuous operation. BLE 5.0 benefits from low power consumption, a high data rate, and low overhead, resulting in the lowest energy consumption per bit and very low overall energy consumption. Despite lower energy consumption per bit of ZigBee wireless technology, overall energy consumption rises with larger data sizes due to higher overhead percentage, whereas, LoRaWAN has the highest energy consumption owing to its $E_{T,b}$ is more dominate factor of the energy consumption. Moreover, these technologies excel in different aspects. For example, LoRaWAN is optimal for long-range communication, whereas ZigBee is suitable for mesh networking. Consequently, both

the total number of bits that devices transmit (B_T) and energy consumption per bit ($E_\mathrm{T,b}$) play a role in determining energy cost of data transmission. Once the data reaches the AP is passed to the server for storage and preprocessing.

V. ENERGY COST OF STORAGE AND DATA PREPROCESSING

Typically, data is first stored on a hard drive, subsequently preprocessed, and then used for the ML model development. In the following, we consider the dataset with N_S samples collected via wireless transmissions as depicted in Figure 1 and discussed in Section IV.

A. Storage

The energy consumption of storage primarily depends on the type of hard drive. According to [36], a typical hard drive consumes 0.65 Watt-Hour per Terabyte stored with a hard disk drive (HDD)-based technology. On the other hand, solid state drive (SSD)-based hard drive consumes 1.2 Watt-Hour per Terabyte. For example, the energy consumption (E_storage [J]) of a dataset with $N_\mathrm{S} = 256$ samples in the form of double-precision floating number consumes 4.79×10^{-6} and 8.85×10^{-6} Joules for HDD and SSD-based technology, respectively, whereas the corresponding energy consumption per bit ($E_\mathrm{storage,b}$ [J/b]) are 2.92×10^{-10} and 5.4×10^{-10}.

B. Data preprocessing

We consider a data preprocessing approach consisting of *data cleaning* and *data standardization* steps, while we leave other more complex approaches such as feature engineering and transformations to future work. We assume that the data-cleaning process is performed in two steps. The first step is identifying and removing invalid samples from a list or array which incurs 0 FLOP since no floating points additions and multiplications are performed, only comparisons and memory operations. The second step is to determine the complexity of data standardization (M_DS). We provide two examples, i.e., min-max scaling and normalization process, both representing a standard approach for data standardization.

Algorithm 1 Min-Max scaling

1: **Initial** min_value and max_value as $data[0]$
2: **for** $i = 1$ **to** $N_\mathrm{S} - N_\mathrm{NaN} - 1$ **do**
3:     **if** $data[i] < min\_value$ **then**
4:         $min\_value \leftarrow data[i]$
5:     **end if**
6:     **if** $data[i] > max\_value$ **then**
7:         $max\_value \leftarrow data[i]$
8:     **end if**
9: **end for**
10: $range\_value \leftarrow max\_value - min\_value$
11: **for** $i = 0$ **to** $N_\mathrm{S} - N_\mathrm{NaN} - 1$ **do**
12:     $data[i] \leftarrow (data[i] - min\_value)/range\_value$
13: **end for**
14: **return** $data$

Algorithm 2 Normalization process

1: **Step 1: Calculate Mean**
2: $sum \leftarrow 0$
3: **for** $i = 0$ **to** $N_\mathrm{S} - N_\mathrm{NaN} - 1$ **do**
4:     $sum \leftarrow sum + data[i]$
5: **end for**
6: $mean \leftarrow \frac{sum}{N_\mathrm{S}}$
7: **Step 2: Calculate Standard Deviation**
8: $squared\_deviations \leftarrow 0$
9: **for** $i = 0$ **to** $N_\mathrm{S} - N_\mathrm{NaN} - 1$ **do**
10:     $squared\_deviations \leftarrow squared\_deviations + (data[i] - mean)^2$
11: **end for**
12: $std\_dev \leftarrow \sqrt{\frac{squared\_deviations}{N_\mathrm{S}}}$
13: **Step 3: Normalize Data**
14: **for** $i = 0$ **to** $N_\mathrm{S} - N_\mathrm{NaN} - 1$ **do**
15:     $normalized\_data[i] \leftarrow \frac{data[i] - mean}{std\_dev}$
16: **end for**
17: **return** $normalized\_data$

---

a) Min-max scaling: In this method, which we detail in Algorithm 1, we first initialize two values for the minimum and maximum. Then, we iteratively search for minimum and maximum values by going through all the valid samples to update these values (lines 2 to 9), which involve comparisons but no FLOP. After finding the minimum and maximum values, we calculate the range (line 10), which requires one FLOP. Finally, we scale the dataset (lines 11 to 13) by performing a subtraction and division for each valid sample, costing $2(N_\mathrm{S} - N_\mathrm{NaN} - 1)$ floating-point operations (FLOPs). Therefore, the corresponding total number of FLOPs ($M_\mathrm{DS}^\mathrm{minmax}$) of min-max scaling can be expressed as:

$$M_\mathrm{DS}^\mathrm{minmax} = 2 \cdot (N_\mathrm{S} - N_\mathrm{NaN}) - 1, \qquad (5)$$

where N_NaN is the number of invalid samples.

b) Normalization: Normalization is performed in three steps, as described in Algorithm 2. The algorithm starts by calculating the mean value (lines 2 to 6), followed by the calculation of the standard deviation (lines 8 to 12). Finally, the algorithm iteratively normalizes each sample (lines 14 to 16). Thus, the total operation ($N_\mathrm{DS}^\mathrm{norm}$) can be expressed as:

$$M_\mathrm{DS}^\mathrm{normalization} = 6 \cdot (N_\mathrm{S} - N_\mathrm{NaN} - 1) + 3. \qquad (6)$$

As a result, the total number of FLOPs for preprocessing can be expressed as:

$$M_\mathrm{pre} = \begin{cases} 2 \cdot (N_\mathrm{DS} - N_\mathrm{NaN}) - 1, & \text{if min-max scaling,} \\ 6 \cdot (N_\mathrm{DS} - N_\mathrm{NaN}) - 3, & \text{if normalization.} \end{cases} \qquad (7)$$

We can observe that the *computing complexity of both standardization methods decreases linearly as the number of invalid samples increases. This indicates that a higher number of invalid samples lowers the computing complexity, leading to reduced energy consumption. However, this also means that the application has to request additional transmissions from*
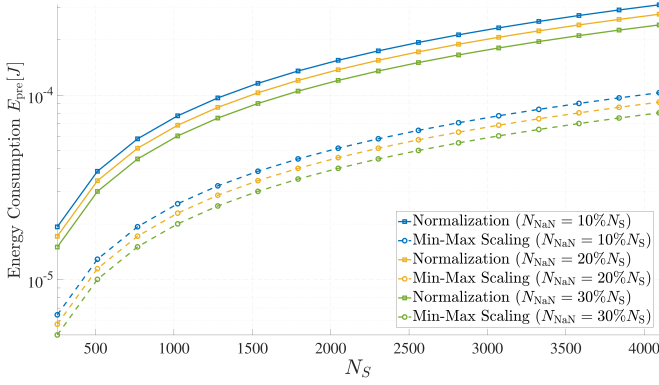
Fig. 5: Energy consumption (E_{pre}) across different number of collected samples (N_{S}) and invalid samples (N_{NaN}).

Fig. 6: Comparison of energy consumption per bit ($E_{\text{pre,b}}$) between Min-Max scaling and normalization.

the device and perform extra operations to preprocess the data on the server.

With the computing complexity in FLOPs formalized, we can obtain total energy consumption (E_{pre}) of the preprocessing (E_{pre}) by utilizing the power consumption of the processing unit and the executing time (T_{pre}). Thus, it is expressed as follows:

$$E_{\text{pre}}[J] = P_{\text{pre}}[W] \cdot T_{\text{pre}}[s], \tag{8}$$

where T_{pre} can be calculated as the ratio between FLOPs needed for preprocessing and the computational power of a processor (N_{PU}).

$$T_{\text{pre}}[s] = \frac{M_{\text{pre}}[FLOPs]}{M_{\text{PU}}[FLOPs/s]}. \tag{9}$$

Consequently, the energy consumption per bit for preprocessing can then be determined as:

$$E_{\text{pre,b}}[J/b] = \frac{E_{\text{pre}}[J]}{\alpha N_{\text{S}}[b]}. \tag{10}$$

For example, the E_{pre} and the corresponding $E_{\text{pre,b}}$ for performing data preprocessing on a CPU with a performance of $M_{\text{PU}} = 10 \ GFLOPs/s$ and consume power of $P_{\text{pre}} = 140 \ W$ can be seen in the Fig. 5 and Fig. 6, respectively. More specifically, Fig. 5 shows that the energy consumption for both standardization methods decreases as the number of invalid samples increases, confirming that higher invalid sample rates lead to lower computational requirements. In addition, Fig. 6 illustrates the energy consumption per bit for normalization and min-max scaling with $N_{\text{S}} = 256$, where normalization consumes three times more energy per bit than min-max scaling. These results highlight the importance of selecting an appropriate preprocessing method based on both the energy efficiency requirements and AI/ML technique requirements. After processing the samples, the training process described in the next section can be carried out.

VI. ENERGY COST OF TRAINING

While there are many AI/ML models available, in this work we focus on a fully connected Multilayer Perceptron (MLP), as
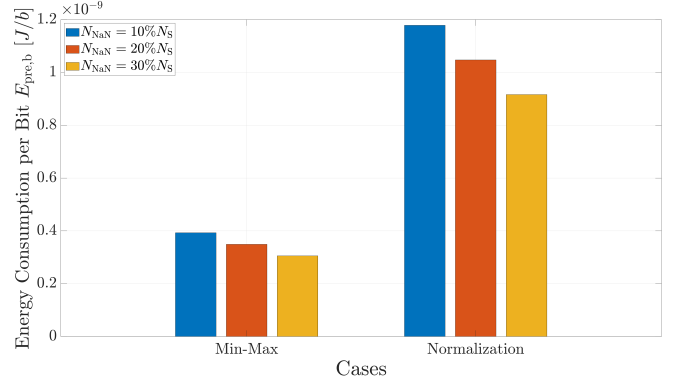
they form the foundation of all modern AI methods and point the reader to works such as [11] for a more comprehensive view on estimating energy consumption in machine learning. A filly connected MLP architecture is depicted in Fig. 7 with the blue and red arrows illustrating the forward and backwards propagation taking place during the training process while the training is summarized in Algorithm 3. The architecture comprises of one input layer with N_{I} neurons, K hidden layers, in each layer it has M neurons and N_{O} neurons in the output layer. As shown in the Fig. 1, the training process includes two steps, namely, training and evaluation. Typically, input samples are split into certain ratios for training and evaluation. For example, with a 70/30 split, a dataset with 256 samples will have 179 samples for training, and 77 samples for evaluation. Therefore, we introduce β for such ratio. More specifically, the input samples can be expressed as:

$$N_{\text{S}} = \underbrace{\beta N_{\text{S}}}_{N_{\text{S,T}}} + \underbrace{(1-\beta)N_{\text{S}}}_{N_{\text{S,E}}}, \tag{11}$$

where $N_{\text{S,T}}$ and $N_{\text{S,E}}$ represent the number of samples for training and evaluation, respectively.

Model training of MLP involves two main phases as depicted in Fig. 7 and Algorithm 3. First, the training samples undergo *forward propagation* where neurons compute
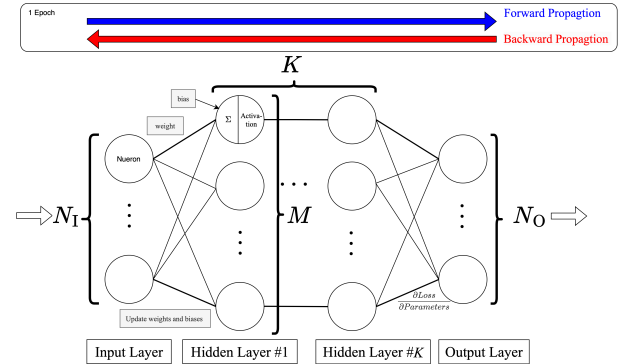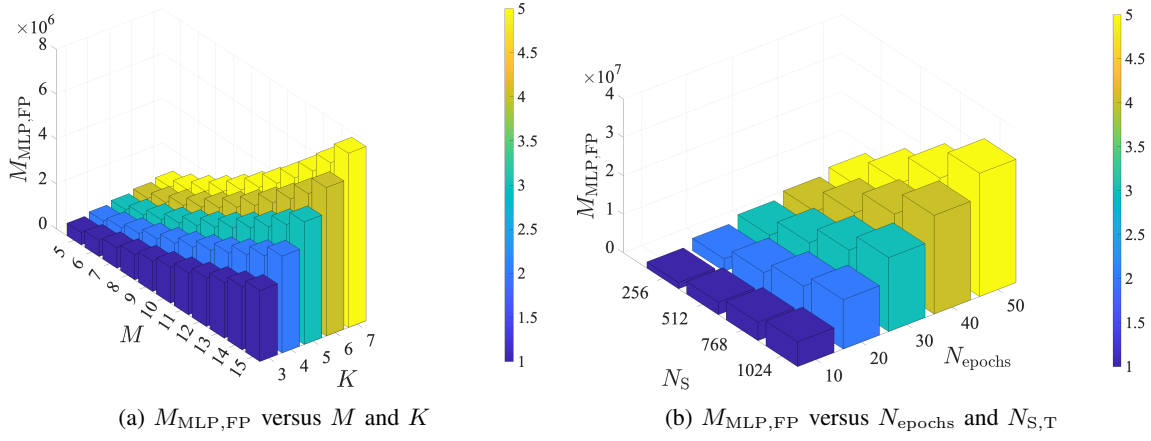

Fig. 7: A fully connected MLP architecture.

(a) $M_{\mathrm{MLP,FP}}$ versus M and K (b) $M_{\mathrm{MLP,FP}}$ versus N_{epochs} and $N_{\mathrm{S,T}}$

Fig. 8: Computational complexity of one forward propagation during training ($M_{\mathrm{MLP,FP}}$) with different parameters.any

---

Algorithm 3 Training an MLP

1: **Initialize** random weights w and biases bias
2: **for** epoch $= 1$ **to** N_{epochs} **do**
3:     Shuffle the dataset
4:     **for** each batch in dataset **do**
5:         **Forward Propagate:**
6:         **for** layer $k = 1$ **to** K **do**
7:             Calculate Linear combination
8:             Apply activation function
9:         **end for**
10:         Compute loss $\mathcal{L}$ for the batch
11:         **Backward Propagate:**
12:         **for** layer $k = K$ **to** 1 **do**
13:             Compute gradient of loss w.r.t. activations $\frac{\partial \mathcal{L}}{\partial a^{(k)}}$
14:             Compute gradient of loss w.r.t. weights $\frac{\partial \mathcal{L}}{\partial w^{(k)}}$
15:             Compute gradient of loss w.r.t. biases $\frac{\partial \mathcal{L}}{\partial \mathrm{bias}^{(k)}}$
16:             Update gradients for next layer $\frac{\partial \mathcal{L}}{\partial a^{(k-1)}}$
17:         **end for**
18:         **Update Weights and Biases:**
19:         **for** layer $k = 1$ **to** K **do**
20:             $w^{(k)} \leftarrow w^{(k)} - \eta \frac{\partial \mathcal{L}}{\partial w^{(k)}}$ (Apply learning rate η)
21:             $bias^{(k)} \leftarrow b^{(k)} - \eta \frac{\partial \mathcal{L}}{\partial \mathrm{bias}^{(k)}}$
22:         **end for**
23:     **end for**
24: **end for**

---

linear combinations of weights and biases, apply activation functions, and calculate the loss between predicted and actual values. Subsequently, the model performs *backward propagation* where it calculates gradients of the loss with respect to each parameter, updates these gradients in reverse through the layers, and adjusts the weights and biases accordingly, which is described in Algorithm 3 from line 11 to line 17. This process completes one epoch. Consequently, we can calculate the energy costs associated with forward and backward propagation, leading to an understanding of the overall energy consumption

for training, subsequently model evaluation, and inference.

A. Computational Complexity of Forward and Backward Propagation

Assuming L layers where $L = K + 2$, the total FLOPs for the forward propagation of a single input sample for an MLP can be expressed as:

$$M_{\mathrm{FP}} = \sum_{l=1}^{L-1} (2 \cdot (M_{l-1} \cdot M_l) + 2 \cdot M_l) \tag{12}$$

where L represents the overall number of layers in the MLP, the first term in the sum represents one multiplication and one addition ($= 2$ FLOPs) related to the weight and bias corresponding to an the edges times the number of edges on that layer ($= M_{l-1} \cdot M_l$) while the second term represents the summation of all the values of the incoming edges and the application of the activation function ($= 2$ FLOPs) times the number of nodes in that layer (M_l). As in our guiding example we assume all hidden layers having the same number of neurons, Eq. 12 becomes $M_{\mathrm{FP}} = (2 \cdot N_{\mathrm{I}} \cdot M + 2 \cdot M) + (2 \cdot (K - 1) \cdot M^2 + 2 \cdot M) + (2 \cdot M N_{\mathrm{O}} + 2 \cdot N_{\mathrm{O}})$ using the notations from Fig. 7. Considering an example MLP with 3 hidden layers with 5 neurons on each hidden layer, 6 neurons on the input layer. Moreover, we aim to train the MLP model and utilize it to make predictions of three-dimensional coordinates based on the input data, thus, there will be 3 neurons on the output layer. Therefore, the total number of FLOPs can be calculated as $M_{\mathrm{FP}} = 2(6 \cdot 5 + 5) + 2(2 \cdot 25 + 5) + 2(5 \cdot 3 + 3) = 226$.

Training consists of multiple epochs and batches. Therefore, the total complexity of forward propagation is:

$$\begin{aligned} M_{\mathrm{MLP,FP}} &= N_{\mathrm{epochs}} \cdot N_{\mathrm{batch}} \cdot \mathrm{batchsize} \cdot M_{\mathrm{FP}} \\ &= N_{\mathrm{epochs}} \cdot N_{\mathrm{S,T}} \cdot M_{\mathrm{FP}}. \end{aligned} \tag{13}$$

Continuing with the example with 256 samples that goes through the aforementioned MLP model across 10 epochs, the computational complexity for forward propagation can be calculated $M_{\mathrm{MLP,FP}} = 10 \cdot 256 \cdot 226 = 578560$ FLOPs as also depicted in Fig. 8a. When all hidden layers have the same

number of neurons and their number M is increasing, it can be seen from Fig. 8a that the FLOPs also increase quadratically. Adding more hidden layers K results in increases more than linearly due to the multiplicative nature of the connections between layers. As per Eq. 13 and Fig. 8b, the relationship between the increase in complexity and the augmentation of the number of samples and epochs is linear. These observations highlight the importance of considering the impact of architectural parameters on the computational complexity of MLP models.

As we can see from Algorithm 3 (line 11 to line 17), the backward propagation consists of approximately twice the computational complexity of forward propagation, which is also confirmed in [37]. Thus, we can approximate the computing complexity of training a model as:

$$M_{\mathrm{MLP}} \approx 3M_{\mathrm{MLP,FP}}. \tag{14}$$

As a result, we can compute the energy consumption for training, model evaluation, and the corresponding energy consumption per bit.

B. Energy Cost of Training

We can obtain the energy consumption of the entire training process as:

$$E_{\mathrm{train}} = \frac{3M_{\mathrm{MLP,FP}}[FLOPs]}{PU_{\mathrm{performance}}[FLOPs/s/W]}, \tag{15}$$

where $PU_{\mathrm{performance}}$ represents the theoretical peak performance of a processing unit. Moreover, the corresponding energy consumption per bit can be obtained from Eq. 15 and the number of input sample, thus, we can show it as:

$$E_{\mathrm{train,b}} = \frac{3M_{\mathrm{FP}}}{\alpha PU_{\mathrm{performance}}}. \tag{16}$$

C. Energy Cost of Model Evaluation

The model evaluation starts once training is complete. This functionality tests the performance of the model on a separate dataset. During the evaluation, the model processes the data using forward propagation without any adjustments to its parameters, which can be seen from lines 5 to 9 in Algorithm 3. Therefore, the energy consumption and energy consumption of model evaluation is expressed as:

$$E_{\mathrm{eval}} = \frac{M_{\mathrm{FP}} \cdot N_{\mathrm{S,E}}}{PU_{\mathrm{performance}}}. \tag{17}$$

By utilizing the same technique as in Eq. 16, the energy consumption per bit of evaluating the model can be expressed as:

$$E_{\mathrm{eval,b}} = \frac{M_{\mathrm{FP}}}{\alpha PU_{\mathrm{performance}}}. \tag{18}$$

VII. ENERGY COST OF INFERENCE

The complexity of making an inference depends on the number of FLOPs required for forward propagating with input sample size $N_{\mathrm{I,P}}$, i.e., $N_{\mathrm{inf}} = M_{\mathrm{FP}} \cdot N_{\mathrm{I,P}}$. For example, when we adopt the aforementioned MLP model with $N_{\mathrm{I,P}} = 77$, the complexity is calculated as $N_{\mathrm{inf}} = 226 \cdot 77 = 17402$ FLOPs.
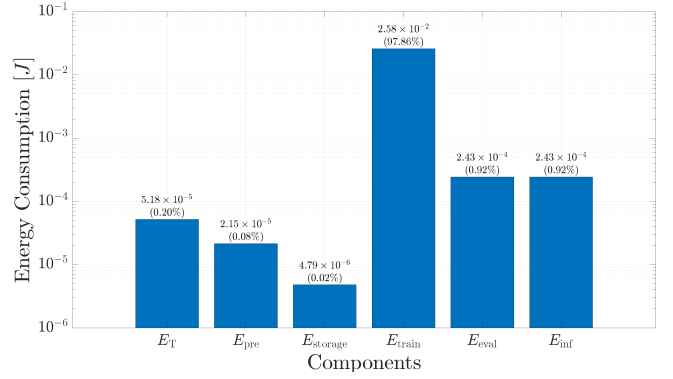

Fig. 9: Comparison of energy consumption in different data manipulation components over the lifecycle of the AIoT model.

Therefore, the energy consumption of the forward propagation and the corresponding inference can be calculated as:

$$E_{\mathrm{inf}} = \frac{M_{\mathrm{FP}} \cdot N_{\mathrm{I,P}}}{PU_{\mathrm{performance}}}. \tag{19}$$

We can then observe *from Eq. 17 and 18, the cost per bit of inference is the same as in evaluation. Thus, we can conclude that the computational complexity between finishing one training and inference is on the magnitude of $3N_{\mathrm{epochs}}N_{\mathrm{S,T}}/N_{\mathrm{I,P}}$. This indicates that the training process involves significantly more computational operations, particularly when the number of epochs or $N_{\mathrm{S,T}} >> N_{\mathrm{I,P}}$. On the other hand, the energy consumption per bit depends on the model complexity and hardware capability. Moreover, the factor of three increases in the energy consumption per bit during training versus inference highlights the additional computational load inherent to training.* Finally, the calculation of end-to-end energy consumption of an AIoT system is presented in the next section.

VIII. ECAL: THE ENERGY COST OF AIoT LIFECYCLE

In this section, we describe the end-to-end energy consumption of an AIoT system for making inferences with a MLP model. First, we consider the energy consumption of developing the model illustrated on the left hand side of Fig. 1 as follows:

$$E_{\mathrm{D}} = E_{\mathrm{T}} + E_{\mathrm{storage}} + E_{\mathrm{pre}} + E_{\mathrm{train}} + E_{\mathrm{eval}}, \tag{20}$$

and the energy consumption per bit that can be expressed as:

$$E_{\mathrm{D,b}} = \frac{E_{\mathrm{D}}}{B_{\mathrm{T}} + \alpha(2N_{\mathrm{S}} + N_{\mathrm{S,T}} + N_{\mathrm{S,E}})}. \tag{21}$$

To compare the energy consumption of all the data manipulation components required to develop and deploy an AIoT system, we continue with the guiding example from the paper where the AI model relies on an an MLP with 3 hidden layers (5 neurons each), whereas on the input layer and output layer there are 6, 3 neurons, respectively, and it requests 256 samples from a IoT device via BLE to train and evaluate

the model with a 70/30 split as discussed in Section VI. In addition, we utilize HDD for storage and normalization as data standardization as discussed in Section V. The energy consumption for this example is shown in Fig. 9 and reveals that the total energy consumed in this scenario is $0.0264J$. Moreover, the energy consumption of a training session is equal to 141 times collecting the same amount of samples from the IoT device, or 71 times of inference. However, these numbers can be significantly higher if the complexity of the model increases or the size of input samples for training is significantly larger than that used for inference as the respective analyses in Sections VI and V showed.

Once the model is developed, it is packaged and deployed in the AIoT system and it can produce inference in the form of continuous or discrete outputs. During its operational lifecycle, the model will be presented some input data and requested to produce the corresponding inference, thus we can express the associated energy cost as:

$$E_{\text{inf,p}} = E_{\text{T}} + E_{\text{storage}} + E_{\text{pre}} + E_{\text{inf}}, \quad (22)$$

it means that we consider the energy cost of inference before the current model needs to be updated. The corresponding energy per bit of inference once deployed is calculated as:

$$E_{\text{inf,p,b}} = \frac{E_{\text{inf,p}}}{B_{\text{T}} + 3\alpha N_{\text{I,P}}}. \quad (23)$$

Next, the entire energy cost over the lifetime of a model in AIoT the energy consumed for the model development, E_{D} is summed with the energy required for performing an inference $E_{\text{inf,p}}$ times the number of times γ the inference is performed with the currently deployed model, and $\gamma \in [1, \infty)$, also referred to as eCAL absolute and measured in $[J]$ as:

$$eCAL_{\text{abs}} = E_{\text{D}} + \gamma E_{\text{inf,p}}. \quad (24)$$

Moreover, the averaged end-to-end energy consumption for one inference can be expressed as:

$$\overline{eCAL}_{\text{abs}} = \frac{eCAL_{\text{abs}}}{\gamma}. \quad (25)$$

As we observe from Eq. 25, *as the number of inferences increases, the average energy consumption decreases and eventually approaches $E_{\text{inf,p}}$, which is depicted in the Fig. 10. This finding can also be utilized to measure how well the model is resilient toward performance loss from an energy consumption point of view. More specifically, with the same hardware setup, a model that requires less frequent retraining due to performance degradation will consume less energy than one that needs frequent retraining.*

Finally, the proposed metric computing the corresponding energy consumption per bit over the lifecycle of the AIoT with the currently deployed model as:

$$eCAL = \frac{eCAL_{\text{abs}}}{B_{\text{T}} + \alpha(2N_{\text{S}} + N_{\text{S,T}} + N_{\text{S,E}}) + \gamma(B_{\text{T}} + 3\alpha N_{\text{I,P}})}. \quad (26)$$
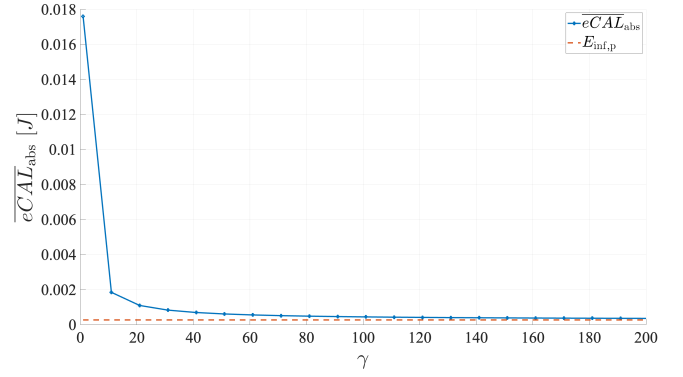

Fig. 10: Average end-to-end energy consumption for one inference ($\bar{E}_{\text{inf,tot}}$) overall number of inference (γ).
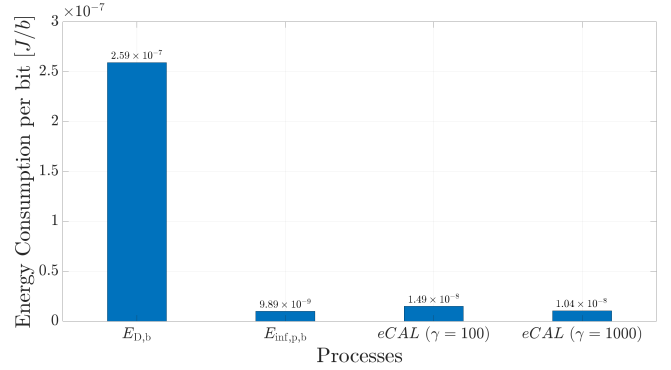

Fig. 11: Comparison of energy consumption per bit in different data manipulation components over the lifecycle of the AIoT model.

To further quantify this relationship, we first compare between Eq. 21, Eq. 23, and Eq. 26, which is depicted in Fig. 11. It shows that the energy consumption per bit of developing the model is $2.59 \times 10^{-7}[J/b]$, which has approximately 26 times higher than the operational lifecycle ($9.89 \times 10^{-9}[J/b]$). Furthermore, we can observe from the figure that the energy consumption per bit decreases with more inferences, dropping from $1.49 \times 10^{-8}[J/b]$ for 100 inferences to $1.04 \times 10^{-8}[J/b]$ for 1000 inferences which is 1.43 times improvement. It is also confirmed in Fig.12, where it follows a similar trend as in Fig.10. More specifically, as the number of the inferences in the current model increases, the energy efficiency of the system also increases.

IX. CARBON FOOTPRINT OF AIoT INFERENCE

The CF is defined as the product of energy consumption and CI, where CI indicates the amount of carbon dioxide equivalents (CO_2eq) emissions associated with generating electrical energy, accounting for all greenhouse gases by weighting each gas by its Global Warming Potential (GWP). This relationship is expressed as:

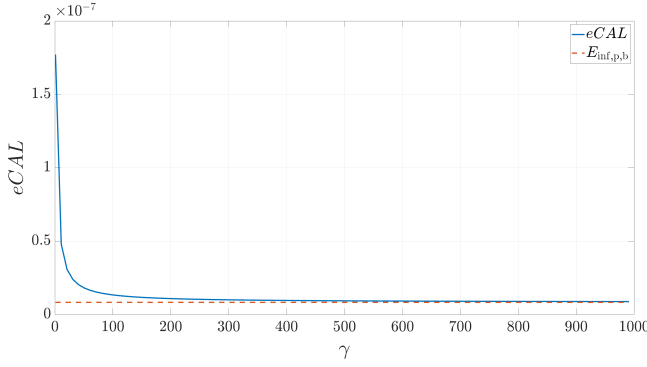$$CF[gCO_2eq] = E[kWh] \cdot CI[gCO_2eq/kWh]. \quad (27)$$

Fig. 12: Energy cost of AIoT lifecycle ($eCAL$) over number of inference (γ).

Fig. 13: Carbon footprint (CF) versus the number of inference (γ) among different countries (based on 2023 data [38]).

TABLE III: CI and CF for end-to-end training and inference in different European countries.

Country	Germany	Ireland	Slovenia	Spain	Finland
Average CI $[gCO_2eq/kWh]$	425	382	239	160	92
CF of end-to-end training $\times 10^{-7}$ $[g]$	20.46	18.39	11.506	7.7025	4.429
CF of inference $\times 10^{-8}$ $[g]$	3.79	3.41	2.13	1.427	0.82

Each country has its own CI, which varies depending on its energy production methods. For example, in 2023, Finland derived 40% of its electricity from hydro and wind sources, with only 10% originating from high CI sources such as coal or gas. This indicates a predominantly low-carbon energy grid. In contrast, Germany, despite utilizing 44% renewable energy, still recorded a relatively high CI [38]. This is attributed to the fact that 38% of its electricity production relied on burning gas, oil, and coal, which are substantial contributors to greenhouse gas emissions. This is shown in Table III, which provides a summary of the average CI values for different countries in 2023, along with the corresponding CF for end-to-end training and inference in an AIoT system. The energy consumption is calculated by utilizing the aforementioned setup, along with Eq. 20 and Eq. 22. We can see that the table reflects the the significant impact of CI on the CF. For example, deploying the same model in Germany results in greenhouse gas emissions that are 4.62 times higher than those in Finland. This highlights the direct correlation between the CI of a country and the environmental cost of technological operations, especially with the integration of AI into the wireless communication systems.

Although the CF for both end-to-end training and inference phases are relatively low, it is important to note that these figures pertain to less complex models and energy-efficient transmission methods. In more realistic scenarios, where models may be more complex and energy demands higher, the CF can substantially increase. Additionally, by considering the total energy consumption in Eq. 24. We can determine how much CO_2 is emitted into the atmosphere in different locations as the number of inferences increases, this is shown in Fig. 13.

The results highlight the significant variation in the CF due to differences in average CI among countries. For example,
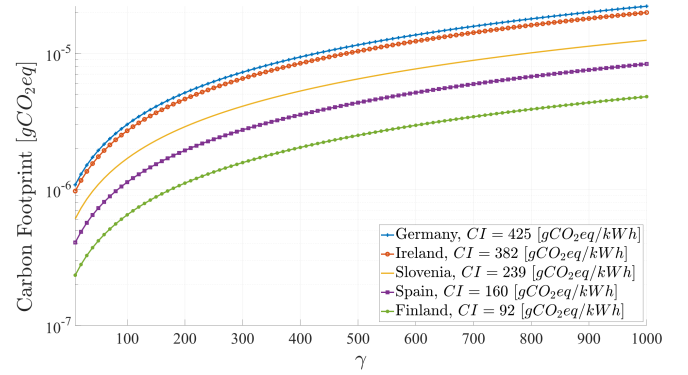
Finland, benefiting from its lowest average CI, exhibits the lowest CO_2 emissions among the five countries analyzed. Therefore, by leveraging lower CI methods to power the system, such as wind or hydro, we can move towards a more sustainable AIoT system.

X. CONCLUSION AND FUTURE WORK

In this work, we proposed a novel metric, namely, eCAL, unlike traditional metrics that focus only on the energy required for transmitting or AI models. It can capture the overall energy cost of generating an inference in an AIoT system during the whole lifecylce of a trained model. We propose a detailed methodology to determine the eCAL of an AIoT system by breaking it down into various data manipulation components, such as data collection, storage, preprocessing, training, evaluation, and inference, and analyzing the complexity and energy consumption of each component. Our proposed metric demonstrates that the more a model is utilized, the more energy-efficient each inference becomes. For example, considering a simple MLP architecture, the energy consumption per bit for 100 inferences is 1.43 times higher than for 1000 inferences. Moreover, we assess the CF of the AIoT system by calculating the equivalent CO_2 emissions based on energy consumption and CI across different countries. Our analysis, using 2023 renewable data, shows that CF varies deploying an AIoT system in different geographic locations, indicating the importance of considering regional energy profiles and their associated CIs in the deployment of AIoT systems.

Through the proposed eCAL metric, this study provides foundations for understanding the energy consumption of AIoT systems. The assumptions are that the model is based on MLPs which are a type of feed-forward neural architectures. Future work may focus on removing that assumption and extend the study to more complex architectures such as recurrent, convolutional, recursive, attention based, etc. and provide a relative complexity comparison of these categories. Furthermore, as virtualization permeates 6G networks, the impact of network slices on the data collection part could be derived. Finally, the development of dynamic energy man-

agement algorithms to optimize the CF in view of a more sustainable operation is relevant.

REFERENCES

[1] M. Arnold, S. Dorner, S. Cammerer, and S. Ten Brink, "On deep learning-based massive MIMO indoor user localization," in *Proc. SPAWC*, Jun. 2018.

[2] M. Khan, B. N. Silva, and K. Han, "Internet of things based energy aware smart home control system," *IEEE Access*, vol. 4, pp. 7556–7566, 2016.

[3] J. Franco, A. Aris, B. Canberk, and A. S. Uluagac, "A survey of honeypots and honeynets for internet of things, industrial internet of things, and cyber-physical systems," *IEEE Commun. Surveys Tuts.*, vol. 23, no. 4, pp. 2351–2383, Aug. 2021.

[4] L. Sanchez, L. Muñoz, J. A. Galache, P. Sotres, J. R. Santana, V. Gutierrez, R. Ramdhany, A. Gluhak, S. Krco, E. Theodoridis, and D. Pfisterer, "SmartSantander: IoT experimentation over a smart city testbed," *Computer Networks*, vol. 61, pp. 217–238, Mar. 2014.

[5] I. Tomar, I. Sreedevi, and N. Pandey, "State-of-art review of traffic light synchronization for intelligent vehicles: Current status, challenges, and emerging trends," *Electronics*, vol. 11, p. 465, Feb. 2022.

[6] H. Moudoud, S. Cherkaoui, and L. Khoukhi, "Towards a scalable and trustworthy blockchain: IoT use case," in *Proc. IEEE ICC*, Jun. 2021.

[7] L. Zhen, A. K. Bashir, K. Yu, Y. D. Al-Otaibi, C. H. Foh, and P. Xiao, "Energy-efficient random access for LEO satellite-assisted 6G internet of remote things," *IEEE Internet of Things J.*, vol. 8, no. 7, pp. 5114–5128, Oct. 2021.

[8] J. Zhang and D. Tao, "Empowering things with intelligence: a survey of the progress, challenges, and opportunities in artificial intelligence of things," *IEEE Internet of Things J.*, vol. 8, no. 10, pp. 7789–7817, Nov. 2020.

[9] P. Dhar, "The carbon impact of artificial intelligence," *Nature Machine Intelligence*, vol. 2, no. 8, pp. 423–425, 2020.

[10] A. S. Luccioni, S. Viguier, and A.-L. Ligozat, "Estimating the carbon footprint of bloom, a 176B parameter language model," *Journal of Machine Learning Research*, vol. 24, no. 253, pp. 1–15, 2023.

[11] E. Garcìa-Martìn, C. F. Rodrigues, G. Riley, and H. Grahn, "Estimation of energy consumption in machine learning," *Journal of Parallel and Distributed Computing*, vol. 134, pp. 75–88, 2019. [Online]. Available: https://www.sciencedirect.com/science/article/pii/S0743731518308773

[12] A. Luccioni, A. Lacoste, and V. Schmidt, "Estimating carbon emissions of artificial intelligence [opinion]," *IEEE Technology and Society Magazine*, vol. 39, no. 2, pp. 48–51, 2020.

[13] A. Faiz, S. Kaneda, R. Wang, R. C. Osi, P. Sharma, F. Chen, and L. Jiang, "LLMCarbon: Modeling the end-to-end carbon footprint of large language models," in *The Twelfth International Conference on Learning Representations*, 2024. [Online]. Available: https://openreview.net/forum?id=aIok3ZD9to

[14] C.-J. Wu, B. Acun, R. Raghavendra, and K. Hazelwood, "Beyond efficiency: Scaling AI sustainably," *IEEE Micro*, 2024.

[15] P. Zhang, Y. Xiao, Y. Li, X. Ge, G. Shi, and Y. Yang, "Toward net-zero carbon emissions in network AI for 6G and beyond," *IEEE Communications Magazine*, vol. 62, no. 4, pp. 58–64, Apr. 2024.

[16] S. Savazzi, V. Rampa, S. Kianoush, and M. Bennis, "An energy and carbon footprint analysis of distributed and federated learning," *IEEE Trans. Green Commun. Netw.*, vol. 7, no. 1, pp. 248–264, Mar. 2023.

[17] X. Hou, J. Liu, X. Tang, C. Li, J. Chen, L. Liang, K.-T. Cheng, and M. Guo, "Architecting efficient multi-modal AIoT systems," in *Proc. 50th Annual International Symposium on Computer Architecture*. New York, USA: Association for Computing Machinery, Jun. 2023. [Online]. Available: https://doi.org/10.1145/3579371.3589066

[18] S. Zhu, K. Ota, and M. Dong, "Energy-efficient artificial intelligence of things with intelligent edge," *IEEE Internet of Things J.*, vol. 9, no. 10, pp. 7525–7532, May 2022.

[19] B. Bertalanič, M. Meža, and C. Fortuna, "Resource-aware time series imaging classification for wireless link layer anomalies," *IEEE Trans. Neural Netw. Learn. Syst.*, vol. 34, no. 10, pp. 8031–8043, 2022.

[20] D. Trihinas, L. Thamsen, J. Beilharz, and M. Symeonides, "Towards energy consumption and carbon footprint testing for AI-driven IoT services," in *Proc. IEEE IC2E*, Sept. 2022, pp. 29–35.

[21] S. L. Jurj, F. Opritoiu, and M. Vladutiu, "Environmentally-friendly metrics for evaluating the performance of deep learning models and systems," in *Proc. ICONIP*. Springer, 2020, pp. 232–244.

[22] C. Naastepad and F. Com, "Labour market flexibility, productivity and national economic performance in five european economies," *Dutch Report, Flexibility and Competitiveness: Labour Market Flexibility, Innovation and Organisation Performance, EU Commission DG Research Contract HPSE-CT-2001-00093*, 2003.

[23] P. Rysavy, "Challenges and considerations in defining spectrum efficiency," *Proceedings of the IEEE*, vol. 102, no. 3, pp. 386–392, 2014.

[24] J. Buberger, A. Kersten, M. Kuder, R. Eckerle, T. Weyh, and T. Thiringer, "Total CO_2-equivalent life-cycle emissions from commercially available passenger cars," *Renewable and Sustainable Energy Reviews*, vol. 159, p. 112158, 2022. [Online]. Available: https://www.sciencedirect.com/science/article/pii/S1364032122000867

[25] D. Barry, A. Danalis, and H. Jagode, "Effortless monitoring of arithmetic intensity with papi's counter analysis toolkit," in *Proc. Tools for High Performance Computing 2018/2019*. Springer, 2021, pp. 195–218.

[26] R. Pereira, M. Couto, F. Ribeiro, R. Rua, J. Cunha, J. P. Fernandes, and J. Saraiva, "Ranking programming languages by energy efficiency," *Science of Computer Programming*, vol. 205, p. 102609, 2021.

[27] S. Farahani, "Chapter 3 - zigbee and ieee 802.15.4 protocol layers," in *ZigBee Wireless Networks and Transceivers*. Burlington: Newnes, 2008, pp. 33–135, accessed: 2024-07-04. [Online]. Available: https://www.sciencedirect.com/science/article/pii/B9780750683937000030

[28] D. Bankov, E. Khorov, and A. Lyakhov, "On the limits of lorawan channel access," in *Proc. IEEE EnT*, Nov. 2016, pp. 10–14.

[29] J. Baliga, R. Ayre, K. Hinton, and R. S. Tucker, "Energy consumption in wired and wireless access networks," *IEEE Communications Magazine*, vol. 49, no. 6, pp. 70–77, 2011.

[30] A. Rayes and S. Salam, *IoT Protocol Stack: A Layered View*. Springer International Publishing, 2022, pp. 97–152. [Online]. Available: https://doi.org/10.1007/978-3-030-90158-5_5

[31] J. Ding, M. Nemati, C. Ranaweera, and J. Choi, "IoT connectivity technologies and applications: A survey," *IEEE Access*, vol. 8, pp. 67 646–67 673, Apr. 2020.

[32] X. Fafoutis, E. Tsimbalo, W. Zhao, H. Chen, E. Mellios, W. Harwin, R. Piechocki, and I. Craddock, "BLE or IEEE 802.15.4: Which home IoT communication solution is more energy-efficient?" *EAI Endors. Trans. Internet Things*, vol. 2, no. 5, Dec. 2016.

[33] "IEEE standard for local and metropolitan area networks–part 15.4: Low-rate wireless personal area networks (LR-WPANs)," *IEEE Std 802.15.4-2011 (Revision of IEEE Std 802.15.4-2006)*, pp. 1–314, 2011.

[34] Semtech Corporation, "LoRa and LoRaWAN: A technical overview," Semtech Corporation, Tech. Rep., 2020, accessed: 2024-07-04. [Online]. Available: https://lora-developers.semtech.com/uploads/documents/files/LoRa_and_LoRaWAN-A_Tech_Overview-Downloadable.pdf

[35] R. Mahapatra, Y. Nijsure, G. Kaddoum, N. Ul Hassan, and C. Yuen, "Energy efficiency tradeoff mechanism towards wireless green communication: A survey," *IEEE Commun. Surveys Tuts.*, vol. 18, no. 1, pp. 686–705, Jan. 2016.

[36] A. Shehabi, S. Smith, D. Sartor, R. Brown, M. Herrlin, J. Koomey, E. Masanet, N. Horner, I. Azevedo, and W. Lintner, "United states data center energy usage report," Lawrence Berkeley National Laboratory, Berkeley, California, Tech. Rep., 2016.

[37] A. G. Baydin, B. A. Pearlmutter, A. A. Radul, and J. M. Siskind, "Automatic differentiation in machine learning: a survey," *Journal of Machine Learning Research*, vol. 18, no. 153, pp. 1–43, 2018. [Online]. Available: http://jmlr.org/papers/v18/17-468.html

[38] Electricity Maps, "Electricity map - slovenia," https://app.electricitymaps.com/zone/SI, accessed: 2024-07-29.